Vol.2, No.1, 12-17 (2010)
http://dx.doi.org/10.4236/ns.2010.21002

Natural Science

Synthesis of nano crystalline spatulae of lead zirconate titanate ($PbZr_{0.52}Ti_{0.48}O_3$)

S. S. Bhatt*, S. C. Chaudhry, Neeraj Sharma, Sonia Gupta

Department of Chemistry, Himachal Pradesh University, Shimla, India; ssbhatt2k@yahoo.com

Received 15 October 2009; revised 29 October 2009; accepted 2 November 2009.

ABSTRACT

A simple and effective method for the synthesis of nano-crystalline PZT spatulae has been reported near MPB via a new *Solution-Ignition Synthesis* route and has been characterized by FT-IR, XRD, TG/DTG/DTA and SEM techniques. X-ray line broadening and Scherrer formula show crystallite size to be~20 nm. Densities of nano-crystalline spatulae of PZT in pellet form made by using 2% PVA and without PVA have been found to be 5.35 and 7.51 gm/cm^3 respectively compared to the theoretical value of 7.78 gm/cm^3. Dielectric constants of 83 and 227 of these spatulae with dielectric loss 0.118 and 0.0609 at 1 MHz and a high resistivity value of 3.043 * 10^7 Ω cm for PZT pellets made without PVA suggest these nano-crystalline PZT spatulae to be the potential candidates for high frequency applications.

Keywords: Nanostructures; Chemical Synthesis; Infrared Spectroscopy; X-ray Diffraction; Dielectric Properties

1. INTRODUCTION

In advanced ceramics technology, the production of good quality powders using different synthetic routes has always been an essential requirement to obtain materials with desired properties, purity and stoichiometry. It is because of an ever-increasing pace of development of various technological innovations to sustain competitive advantage, that various synthetic methods such as self-propagating high temperature synthesis (SHS) [1], sol-gel [2], hydrothermal [3-6], solution combustion synthesis (SCS) [7] and wet grinding solid state thermal reaction (a combination of SHS and SCS methods) [8] have been reported in literature for the preparation of inorganic oxide materials. Metal oxide of composition $PbZr_{0.52}Ti_{0.48}O_3$, synthesized by sintering process between 1200°C and 1300°C is known to be quite important for technological applications due to its ferroelectric and piezoelectric properties near morphotropic phase boundary (MPB) [9,10]. For multilayer components and thick film devices, it is desirable to bring down its sintering temperature, thereby reducing energy consumption and PbO evaporation.

In view of these interesting reports, we have therefore made an attempt to synthesize nano-crystalline spatulae of lead zirconate titanate, $PbZr_{0.52}Ti_{0.48}O_3$, near morphotropic phase boundary (MPB) by a novel method, solution ignition synthesis (SIS). This method is better than other methods in a way that by igniting the solution drop-wise, the surface area is increased and heat produced during ignition is sufficient to rise the internal temperature per ignited drop, thereby reducing the overall high temperature sintering requirement for the ceramics.

2. MATERIALS AND METHODS

2.1. Chemicals

The starting materials used for the preparation of lead zirconate titanate powder i.e. lead acetate $Pb(CH_3COO)_2.3H_2O$, zirconyl nitrate $ZrO(NO_3)_2\ H_2O$ and titanium tetra isopropoxide Ti [$(OPr^i_4]$ were of E Merck and used as such without further purification.

2.2. Preparation of 'As-Ignited Powder'

A solution of lead acetate $Pb(CH_3COO)_2.\ 3H_2O$ (5 gm, 0.0131 mol) in acetic anhydride was added drop-wise to a mixture solution of $ZrO(NO_3)_2.\ H_2O$, (1.5848gm,. 00685 mol) and titanium tetra isopropoxide $Ti(OPr^i)_4$, (1.7984 gm, 0.006326 mol) dissolved in the same solvent, with continuous stirring and a temperature of 60°C during the course of addition was maintained. The resulting clear mixture solution was then ignited by drop-wise addition over aperiod of 4-5 hours into preheated silica crucible kept at 200°C. Yellow colored solid mass formed during the course of addition was scratched from the walls of silica crucible after cooling it to room temperature. It was finally grinded to a fine powder and labeled as "as-ignited powder". The post annealing of the

"as-ignited powder" was done in an electric furnace at 600°C and 700°C for four hours in each case.

2.3. Instrumentation

FTIR spectra were scanned in KBr pellets using single grating Nicolet 5700 series FTIR spectrophotometer in the range of 4000-200 cm^{-1}. Thermal analysis curves (TGA/DTG/DTA) of the synthesized powders were recorded on a double pan SHIMADZU DTG-60H (simultaneous TG/DTA module) thermal analyzer. The thermocouple used was Pt/Pt-Rh (10%) with a temperature range from ambient to 1300°C. The thermal investigations were carried out by heating the sample in a Pt crucible in nitrogen atmosphere and using α-Al_2O_3 as reference. A heating rate of 20°C min^{-1} was employed. The instrument calibration was checked periodically with a sample of $CuSO_4.5H_2O$. Powder X-Ray Diffraction patterns were recorded on PANalytical XPERT-PRO diffractometer system using a typical wavelength of 1.54060 A° (Cu-Kα radiation). The diffraction angle 2θ was varied from 10-70°. The morphology, exact size and shape of the lead zirconate titanate (PZT) particles were determined by recording FESEM of PZT powder annealed at 700°C on Hitachi S-4700 model.

For electrical measurements, two types of pellets, one by using 2% PVA as binder and other without PVA, were made from nano-crystalline PZT spatulae annealed at 700°C. Pelletization was done by applying 15 tons of pressure on nano PZT powder put into a circular dye, from a hydraulic press for 5 minutes and then sintered at 700°C. Both the sides of the sintered pellets were cleaned, smoothened with a very fine sand paper and electroded by applying silver paste. Current Voltage (I-V) measurements were made by using two probe method on Kaithley Source Meter (Model 2611), while dielectric studies were done by measuring capacitance of the sample with metal-insulator-metal (MIM), Agilent 4285A, 75 KHz to 3 MHz precision LCR meter.

3. RESULTS AND DISCUSSION

The synthesis of nano-crystalline PZT powder of composition $Pb(Zr_{0.52}Ti_{0.48})O_3$ near MPB by Solution-Ignition Synthesis has been shown in **Figure 1**.

3.1. FTIR Studies

A perusal of the FTIR spectra of as-ignited PZT powder (**Figure 2a**) shows no absorption bands at 2912cm^{-1}, 1652cm^{-1} and 1560 cm^{-1} attributed to ν_{C-H} and $\nu_{C=O}$ modes of acetate group indicating complete ignition of organic material used for the synthesis of samples. The absorption bands occurring at 1428 cm^{-1} and 1110 cm^{-1}, may be ascribed to ν_{C-O} modes of the trapped atmospheric carbon dioxide in the PZT material [11]. Interestingly, the intensity of these two bands decreases significantly when annealed at 600°C (**Figure 2b**) and disappears completely at 700°C (**Figure 2c**). Another distinct absorption band observed at 563 cm^{-1} has been assigned to ν_{M-O} mode which is characteristic of the formation of ABO_3 type of perovskite structure of PZT powder [12]. The effect of annealing at 600°C and 700°C on the characteristic bands is apparent from the shift of ν_{M-O} band from 563cm^{-1} to higher wave numbers, 590cm^{-1} and 592cm^{-1} respectively, presumably due to increased number of M-O bonds in the perovskite phase of PZT material. In addition, the band at 592cm^{-1} in the sample annealed at 700°C has been found to be more intense than the band at 590cm^{-1} annealed at 600°C, confirming thereby the formation of more of perovskite phase at higher temperature.

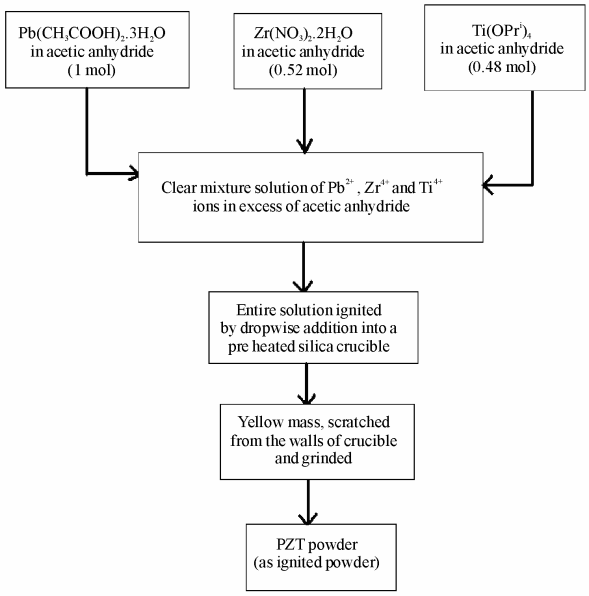

Figure 1. Scheme for the preparation of lead zirconate titanate powder by solution-ignition synthesis (SIS).

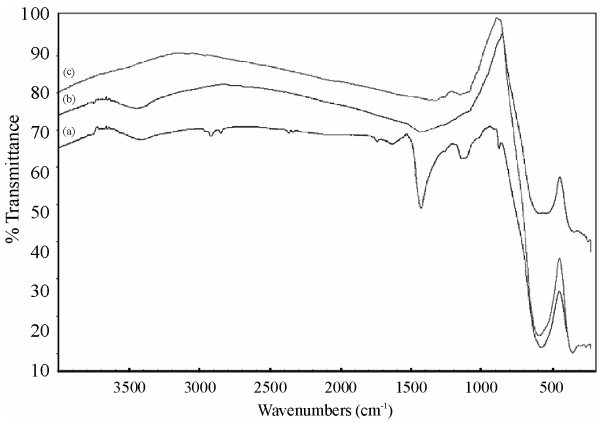

Figure 2. FTIR spectra of a) as-ignited PZT powder; b) powder annealed at 600°C; c) powder annealed at 700°C.

3.2. Thermal Analysis

Thermo analytical curves (TG/DTG/DTA) for as-ignited PZT powder (**Figure 3** blue in color) show only one step decomposition in the range 275.93°C to 331.77°C with a weight loss of only 1.005% as is also substantiated by only one peak in DTG at 311.52°C and an endothermic peak at 307.51°C in DTA curve indicated the escape of carbon dioxide gas trapped in as-ignited PZT powder. The TG/DTA curves (**Figure 3** red in color) of as-ignited powder annealed at 600°C, however, has shown neither any weight loss in TG nor any peak in DTA curve indicating the complete removal of carbon dioxide gas trapped in the lattice of nano-crystalline PZT powder.

3.3. XRD Studies

Powder XRD pattern of as-ignited PZT powder (**Figure 4a**) shows broad and an ordered arrangement of peaks, indicating the formation of nano-crystalline lead zirconate titanate, presumably resulting from the internal heat produced during drop-wise ignition of the reaction mixture solution. Further, the pyrochlore phase which was present initially at 28.5° 2θ with relative intensity of 100% (657 counts) in as-ignited PZT powder (**Figure 4a**) gets significantly reduced at 600°C and completely transformed into perovskite phase at 31.0538° 2θ value after annealing at 700°C (**Figures 4b** and **4c**). Apparently, therefore, the results of the PXRD patterns of as-ignited PZT powder coupled with FTIR and thermo analytical curves suggest that the solution ignition synthesis (SIS) is a novel method of synthesis of nanocrystalline PZT spatulae.

Indexing of the XRD patterns of nano-crystalline PZT powder annealed at 700°C (**Figure 4c**) has been done by matching them with the patterns of known PZT powder of composition $Pb(Zr_{0.52}Ti_{.48})O_3$ [13,14]. Lattice parameters of the sample annealed at 700°C (c=4.32159A° and a=b= 4.06907A°) obtained from (001) and (100) reflections at 20.5522° and 21.8429° 2θ values respectively in XRD pattern with slight lattice distortion (c/a) values to be 1.0620 have been found to be very close to that of 1.066 of pure tetragonal phase [15]. Further, the sharpness of the diffraction peaks in the XRD pattern (**Figure 4c**) suggests better homogeneity and crystallinity of the nano PZT spatulae. It is pertinent to mention here that with the increase in annealing temperature of as-ignited powder from 600°C and finally to 700°C, a substantial increase in the intensity (counts) of the perovskite (110) orientation has been observed thereby confirming the enhanced crystallinity.

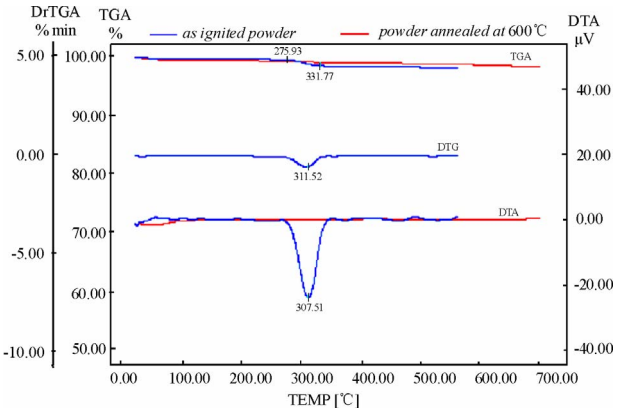

Figure 3. Thermal analysis (TGA/DTA/DTG) curves of as-ignited PZT powder (red) and PZT powder annealed at 600°C (blue).

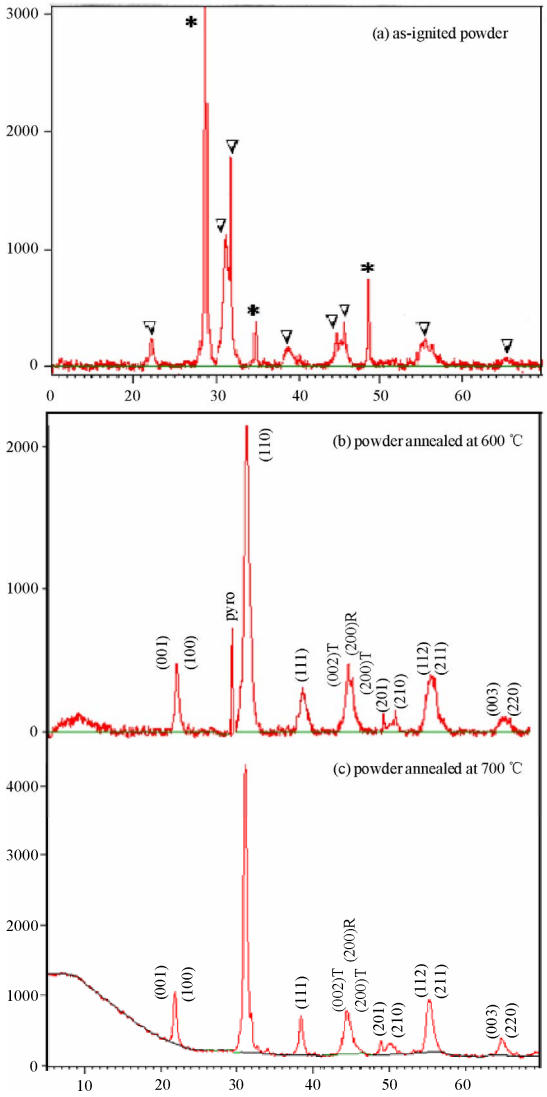

Figure 4. Powder X-ray diffraction patterns of: a) as-ignited PZT Powder; b) PZT powder annealed at 600°C; and c) at 700°C (∇-*Perovskite phase* and ⁎-*Pyrochlore phase*).

The relative amounts of perovskite and pyrochlore phases (**Table 1**) have been determined from the relative intensity of XRD peaks by using following equation [16]:

$$\%\ \text{perovskite phase} = \frac{I_{(110)}}{I_{(110)} + I_{(pyro)}}$$

where $I_{(110)}$-relative intensity of the peak due to (110) orientation and $I_{(pyro)}$-relative intensity of pyrochlore phase. A perusal of the results in **Table 1** indicates that amount of pyrochlore phase decreases while the perovskite phase increases with the increase in annealing temperature.

Apart from the tetragonal phase depicted from the XRD pattern of the PZT powder annealed at 700°C, the relative percentage of rhombohedral and tetragonal phases has been calculated from the triplets of the type (002)T, (200)R and (200)T appearing at 44°-46° 2θ range in the XRD pattern [17] using relation:

$$P_R = \frac{I_{R(200)}}{I_{R(200)} + I_{T(200)} + I_{T(002)}}$$

where P_R represents rhombohedral phase, $I_{R\,(200)}$ is intensity of (200) reflection of rhombohedral phase, $I_{T\,(200)}$ and $I_{T\,(002)}$ is intensity of (200) and (002) reflections of tetragonal phase. The results show that percentage of rhombohedral and tetragonal phase in the present nano-crystalline PZT powder is 30% and 70% respectively indicating thereby that the chemical composition of synthesized nano-crystalline PZT powder lies near to Morphotropic Phase Boundary.

3.4. Crystallite Size, Shape and Density

3.4.1. Size

Broadening of the peaks observed in the XRD patterns (**Figures 4a-4c**) indicates particles in the nano range. Crystallite size of the nano-crystalline PZT powder annealed at 600°C and 700°C has been calculated by using Scherrer Equation i.e.

Table 1. % phases in the nano-crystalline PZT powder samples.

S. No.	Name of Sample	% Perovskite	% Pyrochlore
1	As-ignited powder	36.10	63.89
2	Powder annealed at 600°C	71.81	28.18
3	Powder annealed at 700°C	97.43	2.57

$$\text{Crysttalite size} = \frac{k\lambda}{\beta \cos\theta}$$

where ***k*** is the constant of proportionality (Scherrer constant) and depends on how the width line is determined and value of k is generally taken as 0.9. ***λ*** represents the wavelength of the X rays and has a value of 1.54060A°, ***θ*** is the half of the angle (2θ) of diffraction and ***β*** is the value of broadening of (110) line at Full Width Half Maximum (FWHM) of in radians and has been found to be 13.6 nm which increases to 21.4 nm respectively. Such an increase in the crystallite size with increase in annealing temperature finds support from earlier reports in literature [18,19].

3.4.2. Shape

FESEM of the nano-crystalline PZT powder annealed at 700°C (**Figure 5**) shows a mixture of both spherical particles and stacks of nano spatulae of about 204 nm in width. The spherical nature of the crystallite has been attributed to the high pressure exerted by the evolution of gases such as CO_2, N_2, O_2, etc. during the course of ignition reaction [20] while the formation of stacks of nano spatulae may be attributed to the partial melting and subsequent solidification during dropwise ignition of the PZT powder in the preheated silica crucible.

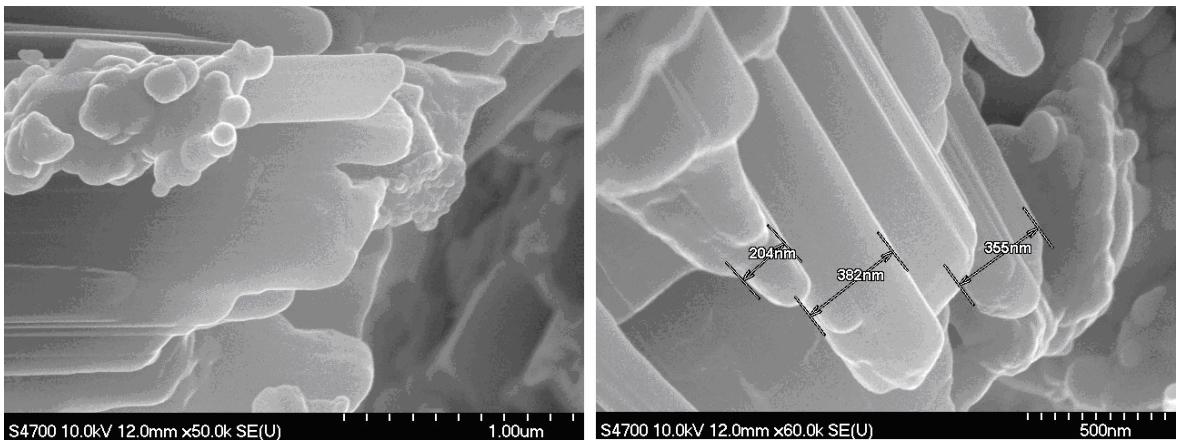

Figure 5. FESEM of nano-crystalline PZT spatulae.

3.4.3. Densities and Porosity

Densities of pellets of nano-crystalline PZT powder (one made with 2% PVA as a binder and other without PVA each of 15 mm in diameter and 1.3 mm thickness) measured by Archimedes Principle have been found to be 5.35 and 7.51 gm/cm^3 respectively. These densities are 68.76% and 96.5% of the theoretical value (7.78 gm/cm^3). The percentage porosity of PZT pellets has been calculated from the relation:

$$\%\ porosity = (1 - \rho/\rho_0) \times 100$$

where **ρ** and **ρ$_o$** are the experimental and the theoretical densities of PZT (7.78 gm/cm^3) and have been found to be 31.24 % and 3.48 %.

3.5. Electrical Properties of Lead Zirconate Titanate of Composition Pb ($Zr_{0.52}Ti_{0.48}$)O_3

3.5.1. D. C. Resistivity

Resistivity has been obtained from current-voltage studies of the pellet prepared from nano-crystalline PZT powder annealed at 700°C by the two probe method using a Keithley Source meter (Model 2611). From a plot of Current vs Voltage (**Figure 6**) resistance 'R' has been calculated from the slope of the plot as, $slope\ (R) = I/V$ and the resistivity 'ρ' using the well known relation, $\rho\ (\text{ohm meter}) = \frac{RA}{d}$ where ***A*** represents the area of the cross section and ***d*** is the thickness of the pellet.

A high resistivity value of 3.043 * 10^7 Ω cm found in the present studies has been attributed to the stoichiometric composition, better crystal structures and improved microstructures obtained by this new solution ignition synthesis (SIS) technique. The higher value of resistivity is also of significant importance as it makes this nano-crystalline PZT spatulae suitable for high frequency application.

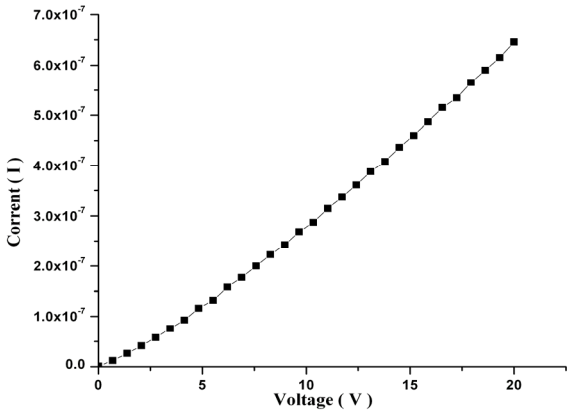

Figure 6. Current (I) vs Voltage (V) plot of nano-crystalline PZT pellet.

3.5.2. Dielectric Studies

The dielectric constant (ε) and dielectric loss (tan δ) of sintered pellets of nano-crystalline PZT spatulae (with 2% PVA and without PVA) as function of frequency at different temperatures have been studied and trends are shown as graphs in **Figures 7a** and **7b**. The values of 83 and 227 for dielectric constant and 0.118 and 0.0609 for dielectric loss have been found at a frequency of 1MHz which remains nearly same in the higher frequency range (up to 3MHz). Further, a comparison of the values of both dielectric constant (227 and 249) and dielectric loss (0.0609 and 0.042) at 298 K and 373 K respectively at constant frequency of 1MHz (**Figure 8**) shows an increase in dielectric constant with decrease in dielectric loss values. These observed low values of dielectric constants have been found to be in agreement with the fact that small grains attain low values of dielectric constant and can stabilize dielectric relaxation up to higher frequency region [21]. These studies also indicate that nano-crystalline spatulae of lead zirconate titanate, Pb ($Zr_{0.52}Ti_{0.48}$)O_3 synthesized near MPB with almost same values of dielectric constant and dielectric loss over a large range of frequencies (up to 3 MHz) may find their role as successful and stable dielectrics in the field of electronics.

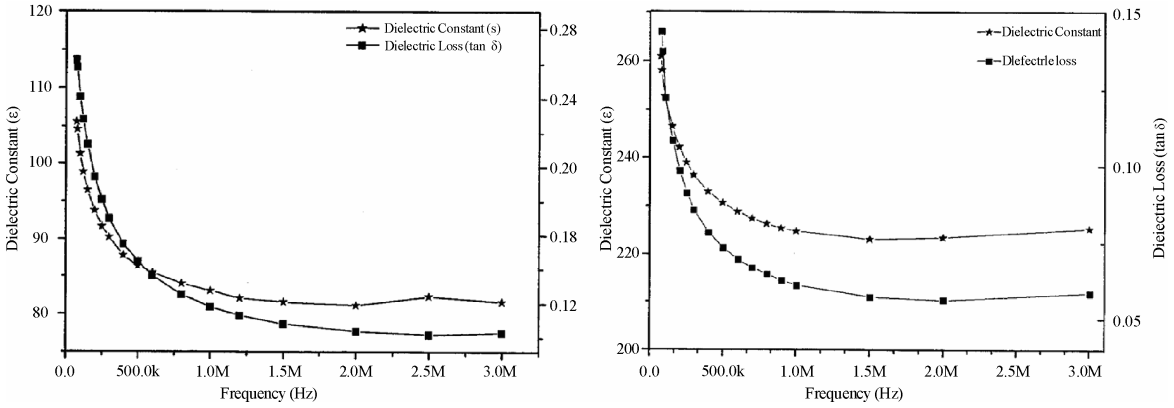

Figure 7. Variation of dielectric constant and dielectric loss with frequency at room temperature for: a) PZT pellet with 2% PVA; and b) PZT pellet without PVA.

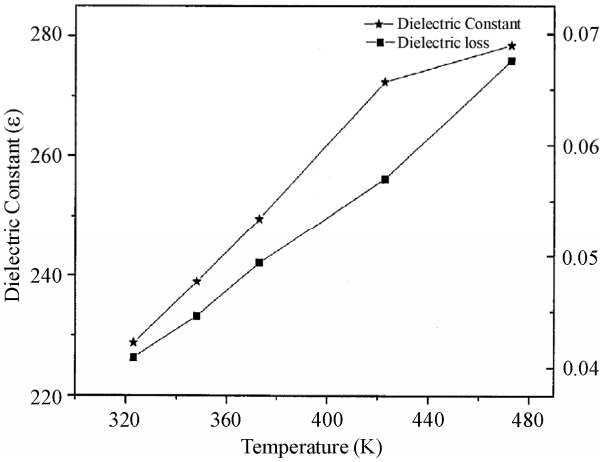

Figure 8. Variation of dielectric constant and dielectric loss with temperature at 1 MHz frequency for PZT pellet without PVA.

4. CONCLUSIONS

The present work describes a simple, effective and novel synthetic strategy namely Solution Ignition Synthesis (SIS) route for the preparation of nano-crystalline PZT, which is advantageous over other commonly employed methods. The FTIR and XRD patterns of the nano crystalline PZT spatulae confirmed their perovskite structure near MPB. The dielectric constant and high values of resistivity also suggest that they may find their role as potential materials suitable for high frequency applications and as stable dielectrics.

5. ACKNOWLEDGEMENTS

The authors wish to acknowledge University Grants Commission, New Delhi and Department of Science and Technology, GOI for providing necessary instrumentation facilities and financial support in the form of SAP and FIST programs to the Department of Chemistry.

REFERENCES

[1] Merzhanov, A.G. (1990) Twenty years of search and findings in combustion and Plasma Synthesis of high temperature materials. Edited by Munir, Z.A. and Holt, J. B., New York VCH Publ. Inc., 1-35.

[2] Livage, J. (1994) The sol-gel route to advanced materials. *Mater. Sc. Forum*, **152 & 153,** 43-54.

[3] Cheng, H.M., Ma, J.M., Zhu, B. and Cui, Y.H. (1993) Reaction mechanisms in the formation of lead zirconate titanate solid solutions under hydrothermal conditions. *J. Am. Ceram. Soc*., **76(3),** 625-629.

[4] Traianidis, M., Courtois, C., Leriche, A. and Thierry, B. (1999) Hydrothermal synthesis of lead zirconium titanate (PZT) powders and their characteristics. *J. Europ. Ceram. Soc*., **12(19),** 1023-1026.

[5] Kutty, T.R.N. and Balachandran, R. (1984) Direct precipitation of lead zirconate titanate by the hydrothermal method. *Mater. Res. Bull*., **19(11),** 1479-1488.

[6] Lencka, M.M., Anderko, A. and Riman, R.E. (1995) Hydrothermal precipitation of lead zirconate titanate solid solutions: thermodynamic modeling and experimental synthesis. *J. Am. Ceram. Soc*., **78(10),** 2609-2618.

[7] Mukasyan, A.S. and Dinka, P. (2007) Novel approach to solution-combustion synthesis of nano-materials. *Int. J. Self Propagating High Temperature Synthesis*, **16(1),** 23-35.

[8] Vijaya, M.S., Senthilkumar, R., Sridevi, K. and Subramnia, A. (2005) Preparation and piezoelectric properties of lead zirconate titanate ceramics. *Ferroelectrics*, **325,** 43-48.

[9] Jaffe, B., Roth, R.S. and Marzullo, S. (1954) Piezoelectric properties of lead zirconate lead titanate solid solution ceramics. *J. Appl. Phys.*, **25,** 809-810.

[10] Kakegawa, K., Mohri, J., Shirasaki, S. and Takahasi, K. (1982) Sluggish pansition between tetragonal and rhombohedral phases of $Pb(Zr,Ti)0_3$ prepared by application of electric field. *J. Am. Ceram. Soc*., **65(10),** 515-519.

[11] Wang, Y. and Jorge, J. (2003) FTIR characterization of PZT nano fibers synthesized from metallo-organic compounds using electro spinning. *Mat. Res. Soc. Symp. Proc*., **736,** D2.9.1-D2.9.6.

[12] Samuneva, B., Jambazov, D., Lepkova, D. and Dimitriev, Y. (1990) Sol-gel synthesis of $BaTiO_3$ and $Ba_{1-x-y}\,a_ySr_x\,Zr_yTi_{1-y})O_3$ perovskite powders. *Ceram. Int*., **16,** 355-360.

[13] Sen, A., Seal, A., Das, N., Mazumdar, R. and Maiti, H.S. (2005) Technological challenges of making PZT based piezoelectric wafers. *Proc. Int. Conf. Smart Mater. Str. Sys*., SC41-SC48.

[14] Kakegawa, K., Mohri, J., Takahashi, T., Yamamura, H. and Shirasaki, S. (1977) Compositional fluctuation and properties of $Pb(Zr,Ti)O_3$. *Powder Diffraction File PDF-2 Database Sets* 1-45*, International Centre for Diffraction Data* (*ICDD*), **24,** 769-772.

[15] Chu, S.Y. and Chen, C.H. (2001) Effect of calcium on the piezoelectric and dielectric properties of Sm-modified $PbTiO_3$ ceramics. *Sensors and Actuators*, **89 (3)**, 210-214.

[16] Lakeman, C.D.E. and Payne, D.A. (1992) Processing effects in the sol gel preparation of PZT dried gels, powders and ferroelectric thin layers. *J. Am Ceram. Soc*., **75,** 3091.

[17] Mishra, S.K., Pandey, D. and Singh, A.P. (1996) Effect of phase coexistence at morphotropic phase boundary on the properties of Pb $(Zr_xTi_{1-x})O_3$ ceramics. *Appl. Phys. Lett.*, **69,** 1707-1709.

[18] Thamjaree, W., Nhuapeng, W. and Tunkasiri, T. (2004) Analysis of X-ray diffraction line profiles of lead zirconate titanate using fourier method. *Ferroelectric Letter*, **31,** 79-85.

[19] Verma, K.C., Kotnala, R.K., Mathpal, M.C., Thakur, N., Gautam, Prikshit and Negi, N.S. (2009) Dielectric properties of nano-crystalline $Pb_{0.8}Zr_{0.2}TiO_3$ thin films at different annealing temperature. *Materials Chemistry and Physics*, **114,** 576.

[20] Nersisyan, H.H., Lee, J.H. and Won, C.W. (2005) SHS of ceramic powders in the fusion salts of alkali metal. *J. Ceram. Process. Res.*, **6(1),** 41-47.

